Article

Not peer-reviewed version

# Genetic Diversity and Molecular Evolution of Porcine Epidemic Diarrhea Virus in Chongqing, China (2022–2024)

Qianlin Chen †, Shaomei Li †, Wenjie Ma, Yassien M. Ibrahim, Dengfeng Xu, Jie Luo, Rui Yang, Hua Zheng, Hao Mu, Liu Yang, Yuandi Yu, Lizhi Fu *, Qingyong Guo *

Posted Date: 1 June 2026

doi: 10.20944/preprints202605.2098.v1

Keywords: porcine epidemic diarrhea virus; epidemiology; S gene; molecular phylogeny; genetic variation

 doi:10.20944/preprints202605.2098.v1



*Article*

# Genetic Diversity and Molecular Evolution of Porcine Epidemic Diarrhea Virus in Chongqing, China (2022–2024)

**Qianlin Chen [1,†], Shaomei Li [2,3,4,5,†], Wenjie Ma [3,4,5], Yassein M. Ibrahim [3,6], Dengfeng Xu [2,3,4,5], Jie Luo [2,3,4,5], Rui Yang [2,3,4,5], Hua Zheng [2,3,4,5], Hao Mu [2,3,4,5], Liu Yang [2,3,4,5], Yuandi Yu [2,3,4,5], Lizhi Fu [2,3,4,5,*] and Qinyong Guo [1,*]**

[1] College of Veterinary Medicine, Xinjiang Agricultural University, Urumqi 830052, China
[2] Chongqing Academy of Animal Science, Chongqing 402460, China
[3] National Center of Technology Innovation for Pigs, Chongqing 402460, China
[4] Rongchang, Animal Disease, Observation and Research Station, Ministry of Agriculture and Rural Affairs, Chongqing 402460, China
[5] Chongqing Engineering Technology Research Center for Veterinary Biological Products, Chongqing 402460, China
[6] Faculty of Veterinary Science, University of Nyala, Nyala 155, Sudan
* Correspondence: flzfulizhi@163.com (L.F.); dygqy@edu.xjau.cn (Q.G.)
† These authors contributed equally to this work.

## Simple Summary

Porcine epidemic diarrhea virus (PEDV) continues to evolve rapidly, while existing vaccines provide limited protection, posing major threats to global swine production. RT-qPCR screening of 296 clinical samples from diarrheic piglets collected in Chongqing between 2022 and 2024 revealed a PEDV positivity rate of 48.31%. Phylogenetic analysis showed that all local strains belonged to the G2c sublineage, and exhibited conserved recombination patterns, distinct COE amino acid substitutions, and variable N-glycosylation sites. These genetic changes may influence viral pathogenicity, antigenicity, and immune evasion capacity, contributing to the continued predominance of the G2c sublineage. This study enhances current PEDV epidemiological data in Southwest China and supports targeted vaccine development.

## Abstract

Porcine epidemic diarrhea virus (PEDV) continues to undergo persistent genetic evolution and remains highly prevalent in pig herds worldwide. The resulting porcine epidemic diarrhea (PED) causes substantial economic losses to the global commercial swine industry. In this study, 296 clinical specimens were collected from diarrheic piglets across nine districts and counties of Chongqing between 2022–2024 and were screened using RT-qPCR. PEDV-positive specimens were detected in all sampling regions, with an overall positive rate of 48.31% (143/296), indicating widespread circulation and endemic persistence of PEDV throughout Chongqing. Phylogenetic analysis of the S gene from 15 representative field isolates revealed that all strains clustered within the G2c sublineage, implying that G2c has become the predominant epidemic lineage circulating in this region in recent years. Sequence analysis showed that the nucleotide identities of the S gene ranged from 93.37%–94.09% compared with the classic CV777 strain and from 96.79%–97.67% compared with the variant AJ1102 strain. Corresponding amino acid similarities were 92.88%–93.56% and 97.25%–98.05%, respectively. Notably, clear recombination footprints were identified in 11 sequenced isolates, all exhibiting highly identical recombination patterns, likely resulting from crossover events between the major parental strain FR/001/2014 and the minor parental strain CH/GDGZ/2012. Furthermore, ten distinct amino acid substitutions including F536L, D566E and L573S were identified within the COE antigenic domain of the S protein, whereas the SS2, SS6 and 2C10 domains remained highly

 doi:10.20944/preprints202605.2098.v1



conserved. Four isolates possessed four novel potential N-glycosylation motifs, including 300 NKTI and 787 NFSV, while two isolates concurrently lost the conserved 341 NLSF glycosylation site. These genetic alterations may influence viral pathogenicity and immune evasion capacity, thereby potentially contributing to the continued predominance and spread of the G2c sublineage in China. Together, this study expands current epidemiological knowledge of PEDV in inland Southwest China, and confirms G2c strains as the dominant circulating variants in local pig populations. These findings provide important molecular insights into the epidemiological trends and evolutionary dynamics of PEDV and offer a valuable reference for the development of more effective prevention and control strategies.

**Keywords:** porcine epidemic diarrhea virus; epidemiology; S gene; molecular phylogeny; genetic variation

## 1. Introduction

Neonatal suckling piglets are highly susceptible to porcine epidemic diarrhea virus (PEDV), which causes acute enteric disease characterized by severe diarrhea, dehydration, and high mortality, with fatality rates approaching 100% in piglets younger than 7 days [1,2]. Porcine epidemic diarrhea (PED) was first reported in the UK in 1971, and the prototype PEDV strain CV777 was subsequently isolated and characterized in Belgium in 1978 [3]. After the first emergence in China in 1984, the PED remained sporadic for several decades [4]. However, the emergence of a highly virulent G2 subgroup in China in October 2010, triggered a nationwide epidemic [5]. In the following years, analogous outbreaks were reported across numerous countries and regions, causing devastating suckling piglet mortalities and substantial economic losses to the global swine sector [6–8]. PEDV is taxonomically classified under the order Nidovirales, family Coronaviridae, genus Alphacoronavirus. It is an enveloped, single-stranded positive-sense RNA virus with an approximately 28 kb genome, containing seven open reading frames (ORFs) arranged as follows: 5'UTR-ORF1a-ORF1b-S-ORF3-E-M-N-3'UTR. ORF1a encodes replicase polyprotein 1a (pp1a). A programmed -1 ribosomal frameshift enables translation read-through from ORF1a into ORF1b, to generate full-length polyprotein pp1ab. This precursor is subsequently cleaved by viral proteases into non-structural proteins nsp1–nsp16. The remaining ORFs sequentially encode spike (S), accessory ORF3, envelope (E), membrane (M), and nucleocapsid (N) proteins [7]. The S, E, and M proteins form the viral envelope, whereas the N protein associates with the genomic RNA to form the nucleocapsid [1].

The S protein, encoded by the S gene, is a type I transmembrane trimeric glycoprotein located on the virion surface. It acts as the key functional molecule mediating host receptor recognition, viral attachment, membrane fusion, and cellular entry [9]. Notably, the S gene is highly variable, and frequently undergoes recombination, substitution, insertion, and deletion events. These genetic changes significantly influence PEDV pathogenicity, transmissibility, and evolutionary dynamics, making the S gene a key target for molecular epidemiological and phylogenetic analyses [10,11]. Based on whole-genome and S-gene homology comparisons, PEDV strains are categorized into classical G1 and variant G2 clades [12]. The G1 clade includes G1a (prototype CV777-like strains) and G1b (early classical isolates such as SD-M). The G2 clade comprises three lineages: G2a (early U.S. field strains such as AH2012), G2b (Chinese epidemic strains from 2010–2020 including AJ1102 and LC), and G2c (recent Chinese variants such as SD2021 and TJbc2023) [13]. Nearly all PED outbreaks reported since 2010 have been linked to G2 variants [14]. This epidemiological shift is likely driven by sustained immune selection pressure resulting from widespread vaccination with strains belonging to G1a (CV777), G1b (ZJ08), and G2b (AJ1102) sublineages. Such pressure accelerates viral evolution, particularly within the S gene, leading to the emergence of novel epidemic strains with altered virulence and transmissibility [15,16]. Despite extensive commercial vaccine use in Chinese swine herds, PEDV prevalence remains high, indicating inadequate cross-protection against currently circulating field strains [17]. Therefore, continuous epidemiological surveillance and

 doi:10.20944/preprints202605.2098.v1



genetic characterization of circulating PEDV variants remain essential for optimizing prevention and control strategies.

To characterize the current epidemiological status and genetic variation of PEDV in inland Southwest China, clinical samples from diarrheic piglets collected across nine districts and counties of Chongqing were analyzed using real-time reverse transcription PCR (RT-qPCR) in the present study. Representative PEDV positive field isolates were subsequently selected for cloning and sequencing to enable detailed genetic characterization and polymorphism analysis. The findings provide valuable data for long-term surveillance of epidemiological trends and evolutionary dynamics of endemic PEDV strains in Chongqing. Furthermore, these findings offer important molecular baseline evidence to support the optimization of integrated PED prevention and control strategies, as well as the development of more effective strain-specific vaccines.

## 2. Materials and Methods

### *2.1. Clinical Samples*

Sample collection was conducted between September 2022 and July 2024. A total of 296 clinical specimens, including intestinal tissue and fecal samples, were collected from piglets clinically suspected of PED, across 18 commercial swine farms located in nine districts and counties of Chongqing (Supplementary Table 1). All sampling procedures were performed by on-site veterinarians with prior consent from farm administrators. The collected specimens were temporarily stored in portable low-temperature biosafety containers, transported to the laboratory under cold-chain conditions, and ultimately maintained at -80 ℃ until further analysis.

### *2.2. Nucleic Acid Extraction*

All stored specimens were retrieved from -80 ℃ freezers and thawed gently on ice to minimize RNA degradation. For fecal specimens, approximately 0.2 g of each sample was transferred into RNase-free 5 mL homogenization tubes, resuspended in 2 mL of pre-chilled RNase-free phosphate-buffered saline (PBS), and thoroughly homogenized using a frozen tissue homogenizer (Shanghai Jingxin Co., Ltd., Shanghai, China) at 60 Hz for 1 min. For intestinal tissue samples, intestinal segments were dissected under chilled conditions. After gently rinsing the tissue surface with pre-chilled PBS to remove contaminants, approximately 0.1 g of intestinal mucosal tissue was collected and placed into 2 mL homogenization tubes containing 1 mL of cold PBS. Samples were homogenized twice at 60 Hz for 1 min, each with a 2 min interval at 4 ℃, to ensure complete tissue lysis and efficient viral release. All homogenate samples were centrifuged at 12,000 rpm for 10 min at 4 ℃, and the clarified supernatants were collected for subsequent viral RNA extraction. Total viral nucleic acids were extracted strictly according to the manufacturer's protocol using an automated nucleic acid extraction instrument (Tianlong Science and Technology Co., Ltd., Xi'an, China). RNA concentration and purity were assessed using the NanoDrop ONE ultramicro spectrophotometer (Thermo Fisher Scientific, Waltham, MA, USA). Qualified RNA samples were aliquoted and stored at -80 ℃ until further molecular analyses.

### *2.3. RT-qPCR Detection*

RT-qPCR detection was performed using a validated assay previously established in our laboratory [18]. Target-specific primers and probes were designed based on the conserved sequence of the PEDV M gene (primer and probe sequences are provided in Supplementary Table 2). All one-step RT-qPCR reactions were conducted on a CFX96™ Real-Time PCR Detection System (Bio-Rad Laboratories, Hercules, CA, USA). The total reaction volume was 20 μL, containing 1 μL of template RNA, 0.5 μM forward primer and 0.3 μM reverse primer. The thermal cycling conditions were as follows: reverse transcription at 52 ℃ for 5 min, followed by initial-denaturation at 95 ℃ for 10 s, followed by 40 amplification cycles consisting of denaturation at 95 ℃ for 5 s and annealing/extension at 61 ℃ for 30 s. Fluorescence signals were captured at the end of each extension cycle. A recombinant

 doi:10.20944/preprints202605.2098.v1



pMD 19T-M plasmid containing the PEDV M gene fragment obtained through double enzyme digestion and gel purification served as the positive control. Negative and blank controls were included in each run to ensure assay reliability. The assay was considered valid when the positive control generated Ct values between 15 and 23, while negative and blank controls showed no specific amplification signals (Ct > 38 or undetectable Ct). Samples with Ct values < 35 were judged as PEDV-positive. To further investigate the genetic characteristics of circulating PEDV strains, representative PEDV-positive intestinal tissue samples from each surveyed region were selected for subsequent S gene amplification, cloning and sequencing analysis.

### *2.4. S Gene Cloning and Sequencing*

Partial amplification primers were designed according to the relatively conserved nucleotide regions within the full-length PEDV S gene, including two pairs of specific primers (PEDV-S1F/PEDV-S1R and PEDV-S2F/PEDV-S2R, primer sequences provided in Supplementary Table 2). Total RNA extracted from positive specimens was reverse-transcribed into first-strand cDNA using the HiScript IV 1st Strand cDNA Synthesis Kit (Vazyme Biotech Co., Ltd., Nanjing, China). The target gene fragments were subsequently amplified by high-fidelity PCR, using 2× Phanta Max Master Mix (Dye Plus, Cat. No. P525, Vazyme Biotech Co., Ltd., Nanjing, China) according to the manufacturer's instructions. Each 20 μL PCR reaction contained 10 μL of 2× Phanta Max Master Mix, 0.5 μM of each forward and reverse primer, and 2 μL of cDNA template. The optimized thermal cycling conditions consisted of an initial denaturation at 95 ℃ for 5 min, followed by 35 cycles of denaturation at 95 ℃ for 15 s, annealing at 60 ℃ for 15 s, and extension at 72 ℃ for 2 min 30 s, with final extension at 72 ℃ for 5 min. PCR products were initially analyzed by 1% agarose gel electrophoresis. DNA bands of the expected sizes were excised and purified using the EasyPure®® Quick Gel Extraction Kit (Cat. No. EG101, TransGen Biotech Co., Ltd., Beijing, China). Purified amplicons were ligated into cloning vectors and transformed into competent cells using the pEASY®®-Blunt Cloning Kit (Cat. No. CB101, TransGen Biotech Co., Ltd., Beijing, China). Positive recombinant colonies were screened by PCR using M13 universal primers. For each valid sample, two confirmed positive clones were selected and submitted to Shanghai Sangon Biotech Co., Ltd. for bidirectional sequencing.

### *2.5. Phylogenetic and Homology Analysis of the S Gene*

Raw sequencing data of S genes amplified from Chongqing-derived PEDV field isolates were assembled and edited using SnapGene software (v8.0), yielding complete full-length S gene sequences. A total of 88 publicly available PEDV reference sequences were retrieved from the NCBI GenBank database (detailed information provided in Supplementary Table 3). Multiple sequence alignment of the obtained full-length sequences and reference strains was performed using MEGA (v11.0) with the MUSCLE algorithm. Based on the aligned datasets, a neighbor-joining (NJ) phylogenetic tree was constructed with 1000 bootstrap replicates to assess branch reliability and annotated and visualized using the Interactive Tree Of Life (iTOL, https://itol.embl.de/) online platform. Sequence homology analysis of the S gene was also performed in MEGA to evaluate the genetic relatedness between local field isolates and representative strains from different PEDV subclusters. Nucleotide and amino acid homology matrices were calculated using the formula [(1-p-distance) × 100%]. The resulting matrix data were imported into RStudio software (v2026.04.0) for the construction of sequence homology heatmaps. A continuous gradient color scale was applied with variations in color intensity representing differences in sequence homology among strains. Additionally, amino acid sequence alignment was performed to compare the major antigenic epitope regions of the S protein, including COE, SS2, SS6, and 2C10, in order to characterize mutation patterns and conservation profiles within these key functional domains.

 doi:10.20944/preprints202605.2098.v1



*2.6. Recombination Analysis*

Potential recombination events in the S gene of Chongqing PEDV strains were analyzed in this study. All sequenced S gene fragments together with representative standard reference sequences were analyzed for recombination using RDP4 software (v4.39). Seven recombination detection algorithms, namely RDP, GENECONV, Chimaera, MaxChi, BootScan, SiScan, and 3Seq, were applied simultaneously using default parameters to ensure comprehensive analysis. Reliable recombination events were considered credible only when at least six of the seven methods identified consistent signals, with a statistical significance threshold of $P < 1.0 \times 10^{-6}$. To further validate the detected recombination events and minimize false-positive results, all candidate recombination signals were subsequently confirmed using SimPlot software (v3.5.1).

*2.7. Analysis of Potential N-Glycosylation Sites on the S Protein*

To characterize the distribution features of putative N-glycosylation sites on the S protein of endemic PEDV isolates from Chongqing, the full-length nucleotide sequences of representative field strains were translated into corresponding amino acid sequences. Potential N-glycosylation sites were predicted using the online NetNGlyc-1.0 platform (https://services.healthtech.dtu.dk/services/NetNGlyc-1.0/) with default parameters. Based on the screening criteria of a prediction score > 0.5 and neural network agreement of at least 7/9, the spatial distribution of predicted N-glycosylation sites was systematically compared between local PEDV variants and representative reference strains from different genetic sublineages.

*2.8. Spatial Analysis of Mutant Amino Acids in the COE Antigenic Domain*

To explore how amino acid substitutions within the COE antigenic domain of local Chongqing PEDV field isolates may alter protein structure and biological function, nucleotide sequences were first converted into their corresponding amino acid sequences. The crystal structure of the prototype CV777 strain (PDB ID: 6VV5) was used as the structural template. ChimeraX software (v1.11.1) was applied to map and visualize mutation sites within the COE domain onto the tertiary structure of the PEDV S protein. Structural superposition was further performed to identify conformational differences induced by site-specific mutations among circulating strains, and to assess their potential functional implications.

## 3. Results

*3.1. RT-qPCR Test Results*

From 2022 to 2024, a total of 296 clinical samples were collected from diarrheic piglets across nine districts and counties of Chongqing, to investigate the regional epidemiological distribution and prevalence characteristics of PEDV. All samples were tested for PEDV using a laboratory-established RT-qPCR assay. Molecular screening revealed an overall PEDV-positive rate of 48.31% (143/296). Notably, PEDV-positive samples were detected in all surveyed regions, with a farm-level positivity rate of 88.89% (16/18). These findings indicate that PEDV has established a widespread epidemic pattern within the swine population of Chongqing. Marked geographic variation in PEDV prevalence was observed among the different sampling regions, with regional positivity rates ranging from 24.32% to 63.33%. Overall, the epidemic intensity exhibited a distinct spatial distribution pattern: central urban areas > southeastern Chongqing Wuling mountainous regions > northeastern Chongqing Three Gorges Reservoir areas. Within the central urban zones, Dazu District exhibited the highest positivity rate (63.33%, 19/30), followed closely by Yongchuan District (61.90%, 26/42). Hechuan and Changshou Districts exhibited comparable infection levels, whereas Rongchang District showed the lowest positivity rate (45.95%, 17/37) within this region. In the southeastern Wuling mountainous area, Shizhu County had the highest PEDV prevalence of 58.33% (14/24), followed by Pengshui County (35.71%, 10/28), while Wulong District demonstrated the lowest

 doi:10.20944/preprints202605.2098.v1



positivity rate (24.32%, 9/37). In the northeastern Three Gorges Reservoir region, Fengdu County, showed PEDV positivity rate of 36.36% (12/33) (Figure 1, Supplementary Table 1).

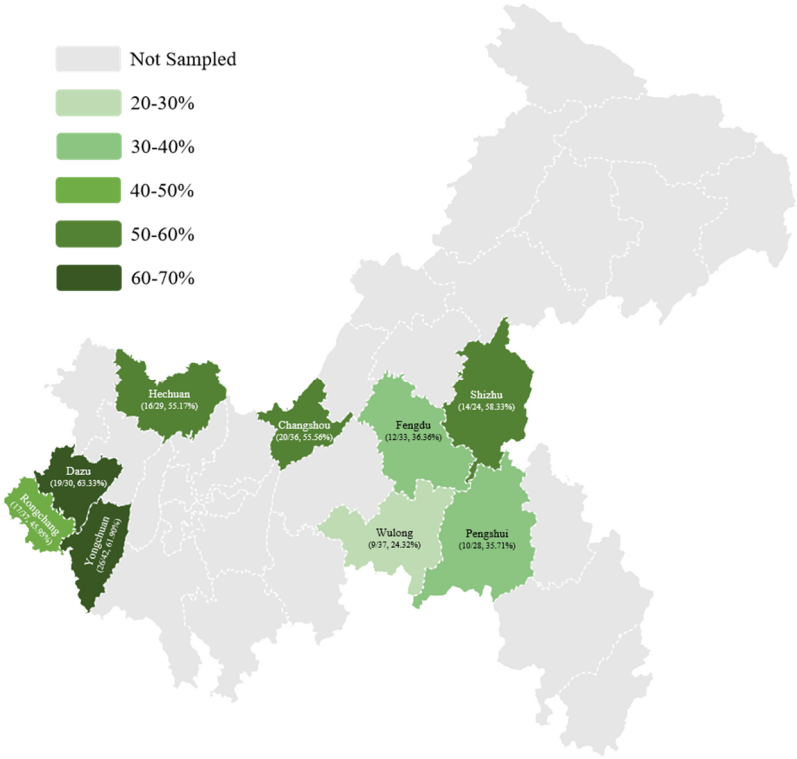


**Figure 1.** Geographic distribution of PEDV-positive specimens in Chongqing. Gray areas represent unsampled administrative regions. The regional PEDV positivity rate was calculated as [(positive samples/total samples) × 100%].

*3.2. Results of S-Gene-Based Phylogenetic Analysis*

To characterize the evolutionary features and dominant genotype distribution of endemic PEDV in Chongqing, 18 PEDV-positive intestinal tissue samples with relatively low Ct values were screened from nine local regions for subsequent molecular analysis. Target fragment amplification was carried out via RT-PCR using S gene-specific primer pairs and high-fidelity DNA polymerase, and all samples successfully yielded amplicons of the expected size. The purified PCR products were cloned into the pEASY®®-Blunt cloning vector and subjected to Sanger sequencing. Raw sequencing reads were assembled with SnapGene v8.0, resulting in 15 full-length S gene sequences with variable nucleotide lengths, including one sequence of 4,149 bp, one of 4,152 bp, four of 4,158 bp, and nine of 4,161 bp. Phylogenetic analysis was performed by aligning the obtained sequences with 88 PEDV reference strains retrieved from the NCBI GenBank database. As shown in Figure 2, all 15 Chongqing field isolates clustered exclusively within the G2c sublineage. This evidence indicates that G2c variants have become the predominant epidemic strains currently circulating in local swine populations. These findings highlight the importance of continuous molecular epidemiological surveillance to enable timely detection and tracking of newly emerging PEDV variants with potential epidemic significance.

 doi:10.20944/preprints202605.2098.v1



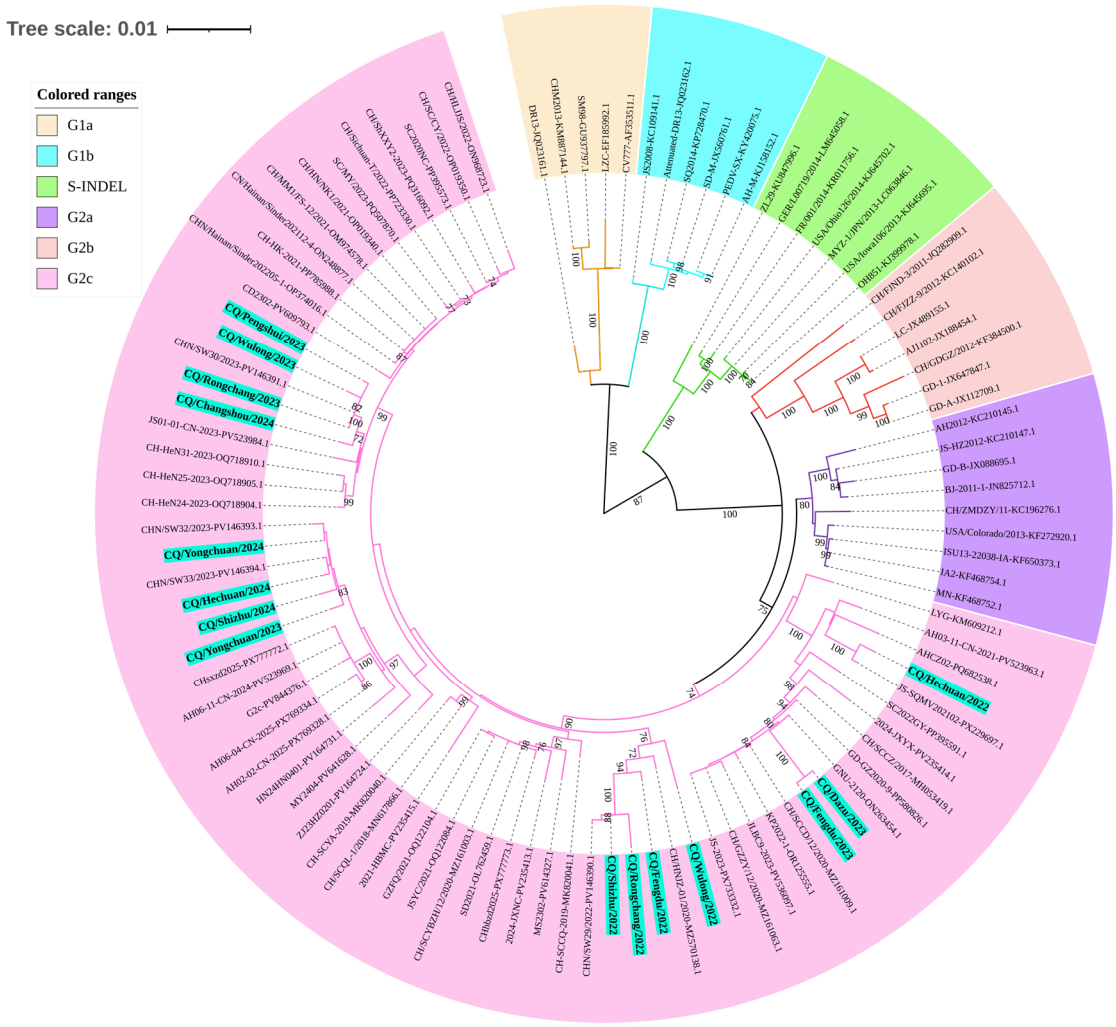


**Figure 2.** Phylogenetic tree based on full-length S gene nucleotide sequences of PEDV. Tree topology was constructed via the neighbor-joining algorithm implemented in MEGA 11.0, with 1000 bootstrap replicates applied to evaluate tree reliability. Only nodal bootstrap values exceeding 70 were displayed. Strain designations and corresponding GenBank accession numbers were annotated on branch terminals. All newly identified Chongqing field strains, marked in bold font with a blue background, were phylogenetically clustered within the G2c sublineage.

### *3.3. Results of S Gene Homology Analysis*

Nucleotide homology analysis of the full-length S gene revealed sequence identities ranging from 97.45% to 99.95% among the 15 PEDV field isolates from Chongqing. Compared with representative strains of different PEDV sublineages, these local isolates shared 93.37%–94.09% nucleotide identity with G1a prototype strain CV777 (AF353511.1), 93.13%–93.97% with the G1b strain SD-M (JX560761.1), and 95.44%–96.33% with the S-INDEL strain OH851 (KJ399978.1). Among G2 reference strains, the obtained sequences exhibited 97.35%–98.51% similarity to the G2a strain AH2012 (KC210145.1), 96.79%–97.67% to the G2b strain AJ1102 (JX188454.1), and 98.07%–98.92% to the G2c representative strain LYG (KM609212.1). In addition, high nucleotide similarity (97.74%–99.90%) was observed with the recently identified Chongqing endemic strain CHN/SW33/2023 (PV146394.1, G2c). The corresponding amino acid sequences were subsequently translated for comparative analysis. The 15 local isolates exhibited 96.60%–99.86% amino acid identity among themselves. Their amino acid similarities to CV777, SD-M, OH851, AH2012, AJ1102, LYG and CHN/SW33/2023 were 92.88%–93.56%, 92.08%–92.83%, 94.42%–95.87%, 96.97%–98.41%, 97.25%–98.05%, 97.33%–98.92% and 97.18%–99.78%, respectively. The nucleotide and amino acid homology relationships between the sequenced isolates and reference strains are presented in the heatmap

 doi:10.20944/preprints202605.2098.v1



(Figure 3, Supplementary Tables 4 and 5). Overall, the Chongqing isolates demonstrated the highest genetic similarity to G2c sublineage strains, particularly to recently circulating regional variants. This indicates that the current PEDV populations in Chongqing are predominantly established within the G2c lineage, and have maintained relatively low genetic divergence in recent years.

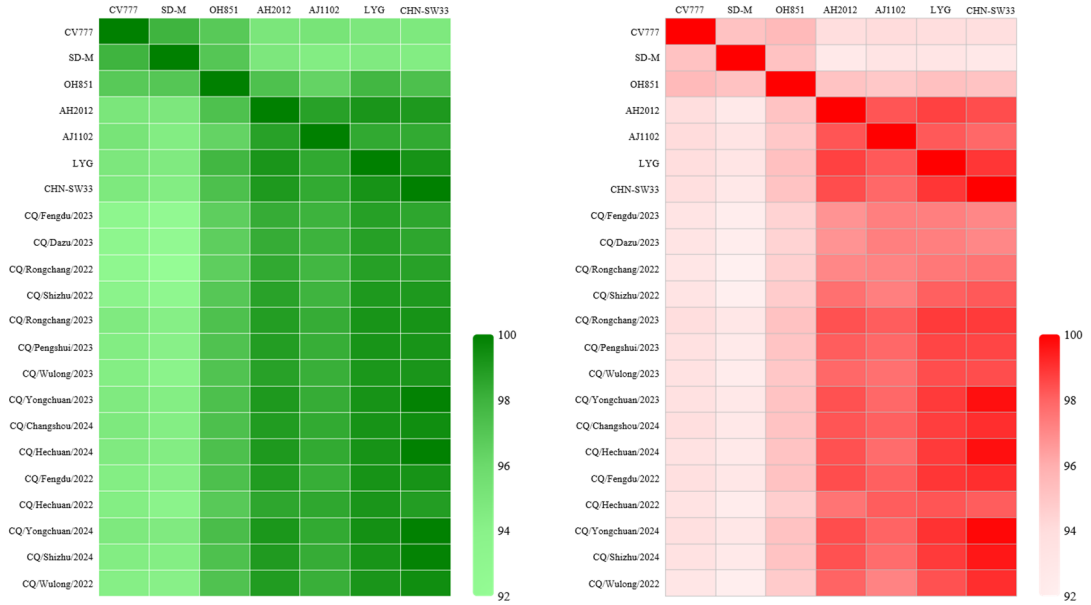


**Figure 3.** Homology heatmap of PEDV based on S gene nucleotide and deduced amino acid sequences. (A) Green blocks represent nucleotide homology between sequenced isolates and reference strains; (B) red blocks indicate amino acid homology.

### *3.4. Comparison of Major Antigenic Epitopes in the S Protein*

Four major antigenic epitopes within the PEDV S protein, including COE (499–638 aa), SS2 (748–755 aa), SS6 (764–771 aa), and 2C10 (1368–1374 aa) [19], were selected for comparative epitope analysis. Sequence variations within these functional domains were evaluated between the Chongqing endemic isolates and seven representative reference strains including CV777, SD-M, OH851, AH2012, AJ1102, LYG, and CHN/SW33/2023. As shown in Figure 4A, ten distinct amino acid substitutions were identified within the COE domain of local PEDV isolates, including S522D/G, F536L, D566E, L573S, L580S, V610A, K621E, E623G, K630I/T and P631S. Notably, residue polymorphism was observed at position 521: two isolates retained leucine consistent with the classical CV777 strain, eight contained histidine matching other sublineage reference strains, four exhibited substitution to arginine, and one carried tyrosine mutation. At residue 594, two local isolates possessed glycine, corresponding to the genotype observed in G1 lineage reference strains. In contrast, SS2, SS6 and 2C10 epitope regions remained highly conserved, with no detectable insertion, deletion or amino acid substitution. To further evaluate the structural implications of these mutations, ChimeraX v1.11.1 was used to map the spatial distribution of prevalent COE substitutions, including A517S, S523G, V527I, T549S, A605E, L612F and I635V (Figures 4B-D). Among these, A517S and T549S are located within the COE domain and may alter internal hydrophobic interactions and local hydrogen bond networks, thereby affecting structural stability. In contrast, V527I, L612F and A605E are positioned on surface-exposed epitope residues, where these substitutions may impair neutralizing antibody recognition and binding. Collectively, these epitope variations imply that contemporary PEDV field strains circulating in Chongqing may possess enhanced potential for immune evasion.

 doi:10.20944/preprints202605.2098.v1



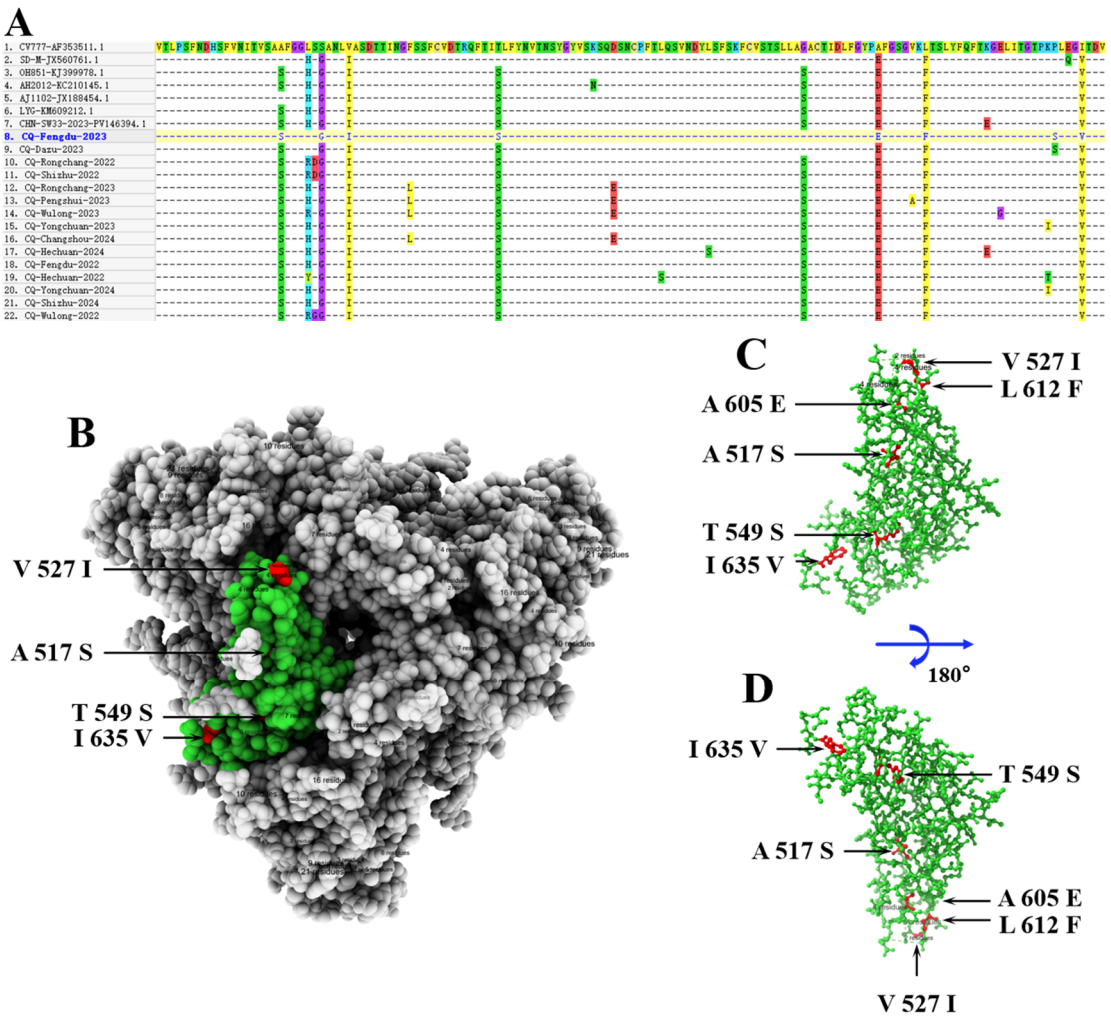


**Figure 4.** Amino acid variation and spatial localization of mutation sites within the PEDV S-protein COE antigenic domain. (A) Multiple sequence alignment of the COE domain sequences from newly acquired Chongqing isolates and seven representative PEDV reference strains, including CV777, SD-M, OH851, AH2012, AJ1102, LYG, and CHN/SW33/2023. (B) Three-dimensional localization of six conserved mutation sites (A517S, V527I, T549S, A605E, L612F, and I635V) mapped onto the resolved S-protein crystal structure of the prototype CV777 strain. (C) Spatial distribution characteristics of the six consensus mutation residues within the COE domain. All mutated sites are highlighted in red: A517S and T549S reside in the COE core functional region; V527I, L612F and A605E are positioned at surface-exposed antigenic epitopes; I635V is situated at the C-terminal marginal region of the COE domain. (D) 180° horizontally rotated view of the COE three-dimensional structural model for comprehensive spatial observation.

### *3.5. Recombination Analysis of S Gene Nucleotide Sequences*

Genetic recombination events within the S gene of newly identified PEDV isolates were screened using RDP4 v4.39. Of the 15 analyzed strains, 11 met the stringent statistical threshold of $P<10^{-6}$ across all seven embedded detection algorithms, confirming robust evidence of recombination. All validated recombinant strains exhibited highly consistent recombination patterns, resulting from genetic exchange between the major parental strain FR/001/2014 (KR011756.1) and the minor parental strain CH/GDGZ/2012 (KF384500.1). Recombination breakpoints were identified within three genomic intervals: 996–4180 nt (six strains), 1112–4180 nt (two strains), and 1293–4180 nt (three strains), with the majority of the recombinant region derived from the major parent FR/001/2014. The remaining four isolates showed weak recombination signals but failed to meet the rigorous screening criteria, therefore excluded from further recombinant analysis. To validate the parental origins and precisely define recombination breakpoints, SimPlot v3.5.1 was subsequently employed. As

 doi:10.20944/preprints202605.2098.v1



illustrated in Figure 5C, strain CQ/Hechuan/2024 exhibited recombination breakpoints at 1141 nt and 2541 nt, which differed slightly from the 1293–4180 nt interval predicted by RDP4. Specifically, the 1–1141 nt region showed greater sequence similarity to the minor parent CH/GDGZ/2012, whereas the downstream region was more closely related to the major parent FR/001/2014. Collectively, these findings demonstrate that natural homologous recombination is a prevalent evolutionary mechanism among contemporary PEDV strains circulating in Chongqing.

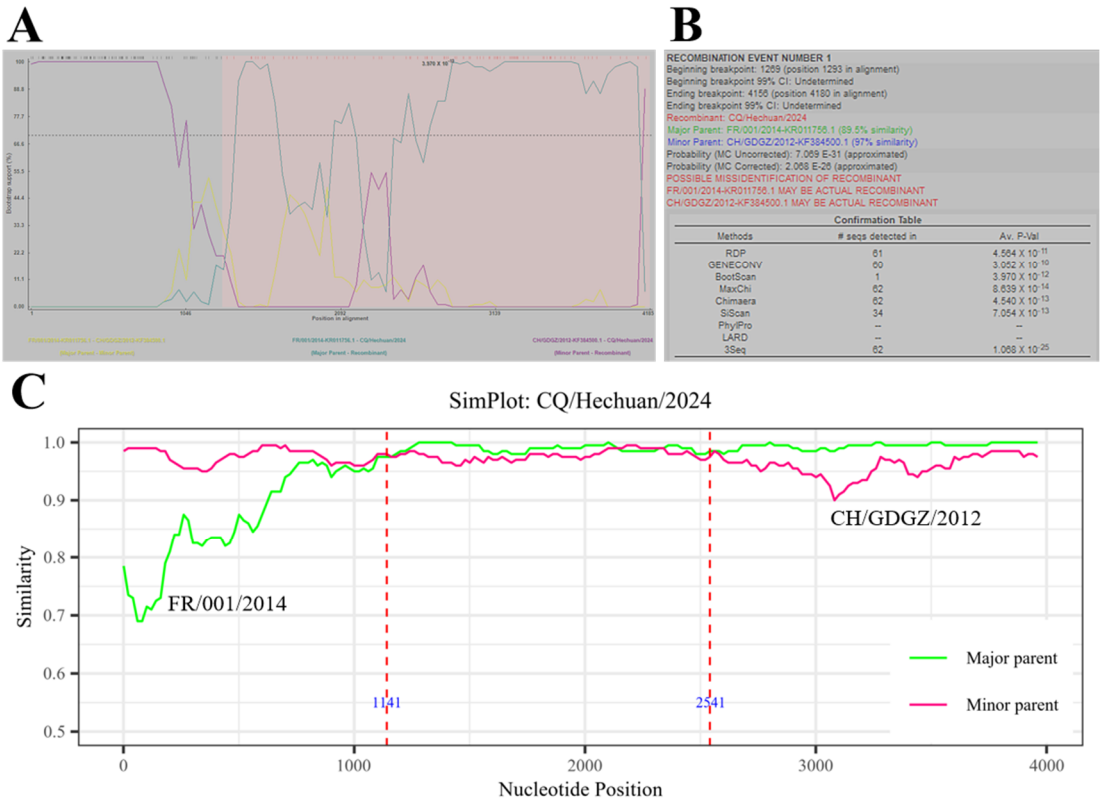


**Figure 5.** Genetic recombination profiling of the S gene from the representative PEDV isolate CQ/Hechuan/2024. (A) Recombination prediction results generated via RDP4 software. The yellow curve represents the sequence similarity between major and minor parental strains; the green curve reflects the homology between the major parent and CQ/Hechuan/2024; the purple curve denotes the genetic similarity between the minor parent and the tested isolate. The pink shaded area delineates the predicted recombinant fragment spanning 1293–4180 nt. (B) Recombination validation based on seven analytical algorithms. A corrected P-value of $2.068\times10^{-26}$ strongly supports the credibility of this intragenic recombination event. (C) Independent verification of recombination breakpoints using SimPlot software. The precise recombination breakpoint was identified at the 1141 nt locus of the CQ/Hechuan/2024 S gene, with FR/001/2014 defined as the major parental strain (green) and CH/GDGZ/2012 as the minor parental strain (magenta).

### *3.6. Prediction of Potential N-Glycosylation Sites on the S Protein*

Potential N-glycosylation sites within the S protein of newly characterized PEDV field isolates were systematically predicted (Table 1). Nine N-glycosylation motifs were highly conserved across PEDV strains from different genetic lineages, including 213 NVTS, 422 NFTG, 511 NITV, 553 NVTN, 685 NVTS, 740 NCTE, 778 NISI, 1246 NKTL, and 1275 NLTG. The preservation of these glycosylation sites indicates that stable N-glycosylation patterns remain relatively stable during the evolutionary progression of endemic PEDV populations. A total of 18-20 putative N-glycosylation sites were identified among the 15 PEDV isolates from Chongqing. Two regional isolates (CQ/Fengdu/2023 and CQ/Dazu/2023) exhibited two novel glycosylation motifs (300 NKTI and 863 NISS) while lacking the canonical 341 NLSF site, a mutation pattern consistent with the minor parental strain CH/GDGZ/2012. In addition, a newly emerged 1196 NRTA site was detected in CQ/Wulong/2023 and

 doi:10.20944/preprints202605.2098.v1



CQ/Yongchuan/2023, whereas the 787 NFSV motif was exclusively identified in the regional dominant strain CHN/SW33/2023 and three newly sequenced isolates. Notably, four mutation-associated glycosylation sites (300 NKTI, 787 NFSV, 863 NISS, and 1196 NRTA) were absent from all other reference PEDV strains, and may therefore represent unique molecular signatures of currently circulating PEDV variants in Chongqing. Further comparative analysis demonstrated that the 57 NSTW and 112 NATA glycosylation sites of local isolates were highly consistent with those of G2-lineage strains. This finding indicates that the glycosylation profiles of endemic PEDV strains are genetically biased toward G2-type epidemic characteristics. Variations in N-glycosylation site distribution may alter the tertiary structure and glycosylation properties of the S protein. Such structural alterations potentially masking critical antigenic epitopes and reducing the binding efficiency of neutralizing antibodies. These molecular adaptations may ultimately enhance viral immune evasion and contribute to the adaptive evolution of regional PEDV strains.

doi:10.20944/preprints202605.2098.v1



**Table 1.** Potential N-Glycosylation sites in the S protein.

| Legend | Strains | High-specificity *N*-glycosylation sites of S protein | | | | | | | | | | | | | | | | | | | | | | |
|---|---|---|---|---|---|---|---|---|---|---|---|---|---|---|---|---|---|---|---|---|---|---|---|---|
| | | 57 | 112 | 127 | 213 | 230 | 300 | 321 | 341 | 348 | 378 | 422 | 511 | 553 | 685 | 740 | 778 | 787 | 863 | 1006 | 1196 | 1229 | 1246 | 1258 | 1275 |
| | | NSSS | + | NKTL | NVTS | NCTG | + | NDTS | NLSF | NSSD | NSTV | NFTG | NITV | NVTN | NVTS | NCTE | NISI | + | + | NITS | + | NLTS | NKTL | NRTG | NLTG |
| G1a | CV777 | NSSS | - | NKTL | NVTS | NCTG | - | NDTS | NLSF | NSSD | NSTV | NFTG | NITV | NVTN | NVTS | NCTE | NISI | - | - | NITS | - | NLTS | NKTL | NRTG | NLTG |
| G1b | SD-M | NSSS | NTSA | NKTL | NVTS | - | - | - | NLSF | NSSD | - | NFTG | NITV | NVTN | NVTS | NCTE | NISI | - | - | NITS | - | NLTS | NKTL | - | NLTG |
| S-INDEL | OH851 | NSSS | - | NKTL | NVTS | - | - | NDTS | NLSF | NSSD | NSTV | NFTG | NITV | NVTN | NVTS | NCTE | NISI | - | - | NISI | - | NLTR | NKTL | NRTG | NLTG |
| G2a | AH2012 | NSTW | NATA | - | NVTS | - | - | NDTS | NFSF | NSSN | NSTV | NFTG | NITV | NVTN | NVTS | NCTE | NISI | - | - | NITS | - | NLTR | NKTL | NRTG | NLTG |
| G2b | AJ1102 | NSTW | NATA | - | NVTS | - | - | NDTS | - | NSSD | NSTV | NFTG | NITV | NVTN | NVTS | NCTE | NISI | - | - | NITS | - | NLTR | NKTL | NRTG | NLTG |
| G2c | LYG | NSTW | NATA | - | NVTS | - | - | NDTS | NFSF | NSSN | NSTV | NFTG | NITV | NVTN | NVTS | NCTE | NISI | - | - | NITS | - | NLTR | NKTL | NRTG | NLTG |
| Endemic strain | CHN/SW33/2023 | NSTW | NATA | - | NVTS | - | - | NDTS | NLSF | NSSN | NSTV | NFTG | NITV | NVTN | NVTS | NCTE | NISI | NFSV | - | NITS | - | NLTR | NKTL | NRTG | NLTG |
| Major parent | FR/001/2014 | NSSS | - | NKTL | NVTS | - | - | NDTS | NLSF | NSSD | NSTV | NFTG | NITV | NVTN | NVTS | NCTE | NISI | - | - | NITS | - | NLTR | NKTL | NRTG | NLTG |
| Minor parent | CH/GDGZ/2012 | NSTW | NATA | NKTL | NVTS | - | - | NDTS | - | NSSD | NSTV | NFTG | NITV | NVTN | NVTS | NCTE | NISI | - | - | NITS | - | NLTR | NKTL | NRTG | NLTG |
| This study | CQ/Fengdu/2023 | NSTW | NATA | - | NVTS | - | NKTI | NDTS | - | NSSD | NSTV | NFTG | NITV | NVTN | NVTS | NCTE | NISI | - | NISS | NITS | - | NLTR | NKTL | NRTG | NLTG |
| This study | CQ/Dazu/2023 | NSTW | NATA | - | NVTS | - | NKTI | NDTS | - | NSSD | NSTV | NFTG | NITV | NVTN | NVTS | NCTE | NISI | - | NISS | NITS | - | NLTR | NKTL | NRTG | NLTG |
| This study | CQ/Rongchang/2022 | NSTW | NATA | - | NVTS | - | - | NGTS | NLSF | NSSD | NSTV | NFTG | NITV | NVTN | NVTS | NCTE | NISI | - | - | NITS | - | NLTR | NKTL | NRTG | NLTG |
| This study | CQ/Shizhu/2022 | NSTW | NATA | - | NVTS | - | - | NDTS | NLSF | NSSD | NSTV | NFTG | NITV | NVTN | NVTS | NCTE | NISI | - | - | NITS | - | NLTR | NKTL | NRTG | NLTG |
| This study | CQ/Rongchang/2023 | NSTW | NATA | - | NVTS | - | - | NDTS | NLSF | NSSD | NSTV | NFTG | NITV | NVTN | NVTS | NCTE | NISI | - | - | NITS | - | NLTR | NKTL | NRTG | NLTG |
| This study | CQ/Pengshui/2023 | NSTW | NATA | - | NVTS | - | - | NDTS | NLSF | NSSD | NSTV | NFTG | NITV | NVTN | NVTS | NCTE | NISI | - | - | NITS | - | NLTR | NKTL | NRTG | NLTG |
| This study | CQ/Wulong/2023 | NSTW | NATA | - | NVTS | - | - | NDTS | NLSF | NSSD | NSTV | NFTG | NITV | NVTN | NVTS | NCTE | NISI | - | - | NITS | NRTA | NLTR | NKTL | NRTG | NLTG |
| This study | CQ/Yongchuan/2023 | NSTW | NATA | - | NVTS | - | - | NDTS | NLSF | NSSN | NSTV | NFTG | NITV | NVTN | NVTS | NCTE | NISI | NFSV | - | NITS | NRTA | NLTR | NKTL | NRTG | NLTG |
| This study | CQ/Changshou/2024 | NSTW | NATA | - | NVTS | - | - | NDTS | NLSF | NSSD | NSTV | NFTG | NITV | NVTN | NVTS | NCTE | NISI | - | - | NITS | - | NLTR | NKTL | NRTG | NLTG |
| This study | CQ/Hechuan/2024 | NSTW | NATA | - | NVTS | - | - | NDTS | NLSF | NSSN | NSTV | NFTG | NITV | NVTN | NVTS | NCTE | NISI | - | - | NITS | - | NLTR | NKTL | NRTG | NLTG |
| This study | CQ/Fengdu/2022 | NSTW | NATA | - | NVTS | - | - | NDTS | NLSF | NSSD | NSTV | NFTG | NITV | NVTN | NVTS | NCTE | NISI | - | - | NITS | - | NLTR | NKTL | NRTG | NLTG |
| This study | CQ/Hechuan/2022 | NSTW | NATA | - | NVTS | - | - | NDTS | NLSF | NSSN | NSTV | NFTG | NITV | NVTN | NVTS | NCTE | NISI | - | - | NITS | - | NLTR | NKTL | NRTG | NLTG |
| This study | CQ/Yongchuan/2024 | NSTW | NATA | - | NVTS | - | - | NDTS | NLSF | NSSN | NSTV | NFTG | NITV | NVTN | NVTS | NCTE | NISI | NFSV | - | NITS | - | NLTR | NKTL | NRTG | NLTG |
| This study | CQ/Shizhu/2024 | NSTW | NATA | - | NVTS | - | - | NDTS | NLSF | NSSN | NSTV | NFTG | NITV | NVTN | NVTS | NCTE | NISI | - | - | NITS | - | NLTR | NKTL | NRTG | NLTG |
| This study | CQ/Wulong/2022 | NSTW | NATA | - | NVTS | - | - | NDTS | NLSF | NSSN | NSTV | NFTG | NITV | NVTN | NVTS | NCTE | NISI | NFSV | - | NITS | - | NLTR | NKTL | NRTG | NLTG |

**Compared with the prototype strain CV777, "+": Newly identified site; "-": Site not detected. Color key (vs. CV777): conserved N-glycosylation sites (Green); mutated or lineage-specific sites (Yellow); novel sites identified (Blue).**

 doi:10.20944/preprints202605.2098.v1



## 4. Discussion

The emergence and rapid dissemination of novel PEDV variants have severely challenged the sustainable development of China's swine industry since 2010. These newly evolved strains exhibit high pathogenicity, with mortality rates in infected neonatal piglets commonly exceeding 80%, resulting in cumulative economic losses estimated at hundreds of billions of yuan nationwide [20]. Currently, commercial PEDV vaccines based on classical G1 and G2 strains, including both inactivated and live-attenuated formulations, are widely used in domestic pig farms. However, clinical breakthrough PED cases continue to be frequently reported in vaccinated herds with neonatal piglet mortality still ranging from 50% to 100% [21]. This strongly indicates that existing immunization strategies provide insufficient cross-protection against currently circulating field strains. Continuous genetic variation has substantially reshaped the evolutionary dynamics of endemic PEDV populations. Long-term molecular surveillance studies have demonstrated that since 2015, the G2c sublineage has gradually replaced the previously dominant G2a strains and has become the predominant epidemic genotype in swine populations across China [22]. This population-level genotype replacement largely explains the persistent prevalence of PEDV, despite the widespread implementation of routine vaccination programs. In this context, continuous molecular epidemiological surveillance of circulating PEDV variants is urgently required. Such efforts are essential for strengthening precision-based prevention and control strategies and for providing reliable genetic evidence to support the development of next-generation vaccines specifically targeting the currently dominant G2c sublineage strains.

Clinical specimens collected from diarrheic piglets across nine districts and counties of Chongqing during 2022–2024 were tested for PEDV using RT-qPCR assay. PEDV positivity was confirmed in all surveyed areas, with an overall prevalence of 48.31% (143/296). This prevalence was slightly higher than the 40.27% (147/365) recorded in Sichuan Province during 2023–2024, where PEDV circulation was detected in 19 of 20 prefecture level regions [23]. Regional epidemiological investigations in neighboring southwestern provinces have similarly demonstrated widespread PEDV endemicity. A decade-long surveillance study conducted in Yunnan Province from 2013 to 2022 reported PEDV circulation across all 11 administrative regions, with annual positivity rates ranging from 9.64% (62/643) to 41.23% (94/228) [24]. Likewise, provincial surveillance data from Guizhou Province collected between 2017 and 2023 showed PEDV positivity rates ranging from 47.62% to 73.59%, with viral infection identified in all nine surveyed regions [25]. Collectively, these cross-regional epidemiological data strongly demonstrate that PEDV has become a stable, highly prevalent and widely distributed endemic pathogen throughout inland southwestern China. Nationwide molecular surveillance data have confirmed the predominant status of the PEDV G2c sublineage among contemporary viral populations in China. Evolutionary analysis has shown that G2c variants have maintained a relatively high substitution rate of at least 1.38 since 2013. In contrast, the evolutionary rates of G2a and G2b sublineage have gradually declined. This evolutionary advantage has facilitated the widespread replacement of G2a and G2b strains by G2c variants in domestic swine populations since 2015 [22]. Large-scale epidemiological investigations further support this genotype shift. One previous study reported that the prevalence of G2c strains in China reached 87.28% (48/55) during 2020–2021 [26]. Another cross-provincial surveillance study spanning nine Chinese provinces from 2021 to 2024 recorded a G2c prevalence of 69.57% (48/69) [27]. In addition, several recent studies have consistently categorized the majority of currently circulating PEDV strains in China within the G2c genetic cluster [27–29]. Consistent with these nationwide epidemiological trends, all PEDV isolates characterized in the present study were phylogenetically classified into the G2c sublineage. These findings provide further field-based evidence supporting the dominant epidemic role of G2c variants in current PEDV circulating in populations. As the most genetically variable coding region of porcine epidemic diarrhea virus, the S gene is highly prone to diverse genetic variations, including homologous recombination, nucleotide insertion, deletion and point substitution. These intrinsic genetic characteristics enable the S gene to play a central role in

 doi:10.20944/preprints202605.2098.v1



regulating viral transmissibility, pathogenic variation, evolutionary divergence and immune escape potential [30]. In the present study, sequence homology analysis demonstrated that PEDV isolates circulating in Chongqing shared 93.37%–94.09% nucleotide similarity with the classical prototype strain CV777 and 96.79%–97.67% identity with the commercial vaccine strain AJ1102. Even minor nucleotide variations may substantially alter key biological characteristics of PEDV, including pathogenicity, immunogenicity and tissue tropism [31]. Amino acid sequence analysis further confirmed 92.88%–93.56% similarity between local isolates and CV777, and 97.25%–98.05% similarity with AJ1102. Subsequent comparative analysis of four major antigenic epitopes (COE, SS2, SS6 and 2C10) revealed strong sequence conservation within SS2, SS6 and 2C10 domains, with no detectable insertion, deletion or amino acid substitution. In contrast, ten characteristic amino acid substitutions were identified within the COE functional domain, namely S522D/G, F536L, D566E, L573S, L580S, V610A, K621E, E623G, K630I/T, and P631S. Accumulated evidence has proven that site-specific amino acid substitutions can alter the physicochemical properties of viral surface proteins, including charge distribution, hydrophobicity and intramolecular non-covalent interactions. These structural alterations ultimately reducing the binding affinity between viral antigens and host neutralizing antibodies [32]. Mutations occurring within key antigenic domains of the S protein may therefore substantially alter viral antigenicity and neutralization sensitivity, constituting a pivotal molecular mechanism underlying PEDV immune evasion. Nevertheless, the precise molecular cascades linking COE domain mutations to viral immune escape remain poorly understood, which warrants further functional investigations.

Homologous recombination is a major evolutionary mechanism driving genetic diversification in coronaviruses. These recombination events can alter viral pathogenicity and transmission dynamics, while facilitating the adaptive evolution of circulating coronavirus populations [33]. Previous studies have demonstrated that the G2c strain NH-TA2020 originated through genetic recombination between the G2b prototype strain AJ1102 and the S-INDEL-type strain OH851 [34]. In contrast to previously reported recombination patterns, all PEDV field isolates obtained from Chongqing in the present study exhibited highly consistent recombinant characteristics. Recombination analysis confirmed that these regional variants originated from intragenic recombination events, involving the S-INDEL strain FR/001/2014 as the major parental strain and the G2b strain CH/GDGZ/2012 as the minor parental strain. The recombination breakpoints were primarily located within the transitional region between the S1-NTD and S1-CTD domains of the S protein. Notably, the major parent FR/001/2014 contributed the pivotal recombinant genomic fragment that covers the entire COE antigenic domain. This genetic replacement may have reshaped the antigenic properties of recombinant progeny strains, thereby facilitating the continued evolution of circulating PEDV field isolates. Rather than representing random genetic events, this unique regional recombination pattern may reflect an adaptive viral response to long-term immune selection pressure generated by sustained vaccination practices in the field. Collectively, these newly identified recombination events expand the known spectrum of genetic variation among currently circulating PEDV strains in China. Furthermore, these findings suggest that PEDV recombination patterns exhibit obvious geographical specificity, with substantial heterogeneity among viral populations from different epidemic regions.

As the largest structural component of PEDV, the spike (S) protein is categorized as a Class I transmembrane glycoprotein. Located on the viral envelope surface, it contains multiple N-glycosylation sites that are essential for several key viral biological functions [35]. Extensive N-linked glycosylation modifications provide an important structural basis for host cell attachment, membrane fusion mediation, and cytoplasmic replication. The maintenance of functional N-glycosylation machinery is therefore critical for efficient viral proliferation. In the present study, four novel N-glycosylation motifs (300 NKTI, 787 NFSV, 863 NISS, and 1196 NRTA) were identified in a subset of PEDV field isolates from Chongqing. None of these modification signatures were detected in classical reference strains, indicating that they may represent unique molecular features of the local endemic PEDV populations. Variations in the number and distribution of N-glycosylation sites can facilitate

 doi:10.20944/preprints202605.2098.v1



the formation of a glycan shield on the surface of the S protein. Such structural alterations may mask critical neutralizing epitopes, enabling the virus to escape recognition and clearance by the host humoral immune response [36]. Furthermore, amino acid substitutions that generate novel glycosylation sites may alter the tertiary structure of the S protein, potentially affecting critical viral processes such as cellular attachment and membrane fusion. These molecular alterations provide credible mechanistic evidence for understanding the adaptive evolution and enhanced immune evasion strategies adopted by currently circulating PEDV variants in Chongqing.

Vaccination remains the cornerstone for preventing PEDV in commercial swine herds. However, the continuous genetic drift and adaptive evolution of circulating PEDV strains increasingly undermine the protective potency of conventional vaccines, posing substantial obstacles to current immunization programs. Therefore, sustained molecular epidemiological surveillance is essential to enable dynamic monitoring of viral genetic variation and evolutionary trends. At the same time, priority should be given to the development of next-generation vaccines specifically tailored to locally predominant strains, together with the optimization of integrated prevention and control strategies. Such coordinated efforts will provide a stronger theoretical foundation and valuable technical guidance for the standardized and evidence-based management of PEDV endemicity in swine populations.

## 5. Conclusions

In conclusion, this study conducted molecular screening of 296 diarrheic piglet specimens collected from nine regions of Chongqing between 2022 and 2024 using RT-qPCR, revealing a PEDV field positivity rate of 48.31% (143/296). Phylogenetic analysis demonstrated that all locally identified PEDV strains clustered exclusively within the G2c sublineage, sharing 93.37%–94.09% nucleotide homology and 92.88%–93.56% amino acid similarity with the classical CV777 prototype strain. Recombination analysis further indicated consistent recombination patterns among these field isolates, resulting from intragenic recombination between the S-INDEL lineage strain FR/001/2014 and the G2b sublineage strain CH/GDGZ/2012. Additionally, mutation profiling identified ten distinct amino acid substitutions concentrated within the critical COE antigenic region of the S protein, along with four novel N-glycosylation sites identified in a subset of regional isolates. Collectively, these findings provide comprehensive S-gene-based evidence of the ongoing evolution of PEDV and clarify the current epidemiological distribution and unique genetic characteristics of the predominant G2c sublineage circulating in Chongqing. These data enrich the regional PEDV genetic database, and provide scientific evidence to support long-term molecular epidemiological monitoring, optimized prevention and control strategies, and the development of next-generation vaccines targeting currently circulating PEDV variants.

**Supplementary Materials:** The following supporting information can be downloaded at the website of this paper posted on Preprints.org.

**Author Contributions:** Conceptualization, Q.C., S.L. and L.F.; methodology, Q.C., W.M. and S.L.; formal analysis, Q.C., S.L., Y.M. and J.L.; investigation, Q.C., D.X., H.M., R.Y. and H.Z.; resources, S.L., L.Y. and Y.Y.; data curation, Q.C., J.L. and S.L.; writing—original draft preparation, Q.C., S.L. and W.M.; writing—review and editing, Y.Y., Q.G. and L.F.; supervision, Q.G. and L.F. All authors have read and agreed to the published version of the manuscript.

**Funding:** This research was funded by the Natural Science Foundation of Chongqing (CSTB2025NSCQ-GPX1047); Chongqing Municipal Financial Grant Project (25524C); National Center of Technology Innovation for Pigs (NCTIP-XD/B19); Observation and Research on Basic and Long-term Agricultural Scientific and Technological Work (MARA-ORS261-AH024); and the Chongqing Special Postdoctoral Science Foundation (25B3N01).

**Institutional Review Board Statement:** Not applicable.

 doi:10.20944/preprints202605.2098.v1



**Informed Consent Statement:** Not applicable.

**Data Availability Statement:** Data is contained within the article or supplementary material.

**Acknowledgments:** Special thanks to my supervisor for his guidance and valuable advice. I sincerely thank all lab colleagues for their help. Finally, I would like to thank all reviewers and editors for their careful review and constructive suggestions.

**Conflicts of Interest:** The authors declare no conflicts of interest.

## References

1. Jung, K.; Saif, L.J.; Wang, Q. Porcine epidemic diarrhea virus (PEDV): An update on etiology, transmission, pathogenesis, and prevention and control. Virus Res, 2020, 286: 198045. DOI: 10.1016/j.virusres.2020.198045
2. Wang, Q.; Vlasova, A.N.; Kenney, S.P.; et al. Emerging and re-emerging coronaviruses in pigs. Curr Opin Virol, 2019, 34: 39-49. DOI: 10.1016/j.coviro.2018.12.001
3. Pensaert, M.B.; de Bouck, P. A new coronavirus-like particle associated with diarrhea in swine. Arch Virol, 1978, 58(3): 243-247. DOI: 10.1007/BF01317606
4. Xuan, H.; Xing, D.; Wang, D.; et al. Study on the culture of porcine epidemic diarrhea virus adapted to fetal porcine intestine primary cell monolayer. Chin. J. Vet. Sci., 1984, 4: 202–208. (In Chinese)
5. Wang, J.; Zhao, P.; Guo, L.; et al. Porcine epidemic diarrhea virus variants with high pathogenicity, China. Emerg Infect Dis, 2013, 19(12): 2048-2049. DOI: 10.3201/eid1912.121088
6. Cima, G. PED virus reinfecting U.S. herds. Virus estimated to have killed 7 million-plus pigs. J Am Vet Med Assoc, 2014, 245(2): 166-167. PMID: 25115019
7. Lee, C. Porcine epidemic diarrhea virus: An emerging and re-emerging epizootic swine virus. Virol J, 2015, 12: 193. DOI: 10.1186/s12985-015-0421-2
8. Ojkic, D.; Hazlett, M.; Fairles, J.; et al. The first case of porcine epidemic diarrhea in Canada. Can Vet J, 2015, 56(2): 149-152. PMID: 25694663
9. Chambers, P.; Pringle, C.R.; Easton, A.J. Heptad repeat sequences are located adjacent to hydrophobic regions in several types of virus fusion glycoproteins. J Gen Virol, 1990, 71(Pt 12): 3075-3080. DOI: 10.1099/0022-1317-71-12-3075
10. Stott, C.J.; Temeeyasen, G.; Tripipat, T.; et al. Evolutionary and epidemiological analyses based on spike genes of porcine epidemic diarrhea virus circulating in Thailand in 2008-2015. Infect Genet Evol, 2017, 50: 70-76. DOI: 10.1016/j.meegid.2017.02.014
11. Zhao, Y.; Fan, B.; Song, X.; et al. PEDV-spike-protein-expressing mRNA vaccine protects piglets against PEDV challenge. mBio, 2024, 15(2): e0295823. DOI: 10.1128/mbio.02958-23
12. Huang, Y.; Dickerman, A.W.; Piñeyro, P.; et al. Origin, evolution, and genotyping of emergent porcine epidemic diarrhea virus strains in the United States. mBio, 2013, 4(5): e00737-13. DOI: 10.1128/mBio.00737-13
13. Su, M.; Li, C.; Qi, S.; et al. A molecular epidemiological investigation of PEDV in China: Characterization of co-infection and genetic diversity of S1-based genes. Transbound Emerg Dis, 2020, 67(3): 1129-1140. DOI: 10.1111/tbed.13439
14. Zhang, Y.; Chen, Y.; Zhou, J.; et al. Porcine Epidemic Diarrhea Virus: An Updated Overview of Virus Epidemiology, Virulence Variation Patterns and Virus-Host Interactions. Viruses, 2022, 14(11). DOI: 10.3390/v14112434
15. Sun, J.; Cheng, J.; Shi, D.; et al. Genetic Epidemiology of Porcine Epidemic Diarrhea Virus Circulating in China From 2010 to 2024: Characterization of Phylogenetic and Genetic Diversity of S1-Based Genes. J Med Virol, 2025, 97(2): e70198. DOI: 10.1002/jmv.70198
16. Zhang, H.; Zou, C.; Peng, O.; et al. Global Dynamics of Porcine Enteric Coronavirus PEDV Epidemiology, Evolution, and Transmission. Mol Biol Evol, 2023, 40(3). DOI: 10.1093/molbev/msad052
17. Fu, Y.; Wang, Y.; Dai, L.; et al. Evolutionary dynamics and antigenic diversity of porcine epidemic diarrhea virus (PEDV) in China: phylogenetic and recombination analyses based on large-scale S gene sequences. BMC Vet Res, 2025, 21(1): 426. DOI: 10.1186/s12917-025-04873-y

 doi:10.20944/preprints202605.2098.v1




18. Chen, Q.; Li, S.; Zhang, Y.; et al. Development of a triplex quantitative reverse transcription-polymerase chain reaction for the detection of porcine epidemic diarrhea virus, transmissible gastroenteritis virus, and porcine delta coronavirus. Chin. J. Vet. Sci., 2025. https://link.cnki.net/urlid/22.1234.R.20250107.1115.002. (In Chinese)
19. Chang, S.; Bae, J.; Kang, T.; et al. Identification of the epitope region capable of inducing neutralizing antibodies against the porcine epidemic diarrhea virus. Mol Cells, 2002, 14(2): 295-299. PMID: 12442904
20. Sun, R.; Cai, R.; Chen, Y.; et al. Outbreak of porcine epidemic diarrhea in suckling piglets, China. Emerg Infect Dis, 2012, 18(1): 161-163. DOI: 10.3201/eid1801.111259
21. Park, J. Porcine Epidemic Diarrhea: Insights and Progress on Vaccines. Vaccines (Basel), 2024, 12(2): 212. DOI: 10.3390/vaccines12020212
22. Gao, M.; Liu, Y.; Xu, X.; et al. Temporal evolutionary dynamics of porcine epidemic diarrhea virus in China from 2013 to 2023. Infect Genet Evol, 2026, 141: 105938. Doi:10.1016/j.meegid.2026.105938.
23. Xiao, L.; Kang, R.; Wu, X.; et al. Prevalence and S gene characterization of porcine epidemic diarrhea virus in Sichuan province, China (2023-2024). Front Vet Sci, 2025, 12: 1748998. DOI: 10.3389/fvets.2025.1748998
24. Zhu, P.; Yuan, H.; Shu, X.; et al. Epidemiological Study and Genetic Diversity Assessment of Porcine Epidemic Diarrhea Virus (PEDV) in Yunnan Province, China. Viruses, 2025, 17(2): 264. DOI: 10.3390/v17020264
25. Tian, H.; Liu, J.; Liang, H.; et al. Epidemiological investigation on the prevalence of PEDV and PoRVA in Guizhou during 2017-2023 and genetic evolution analysis of VP7 and VP4 genes of PoRVA strains. Chin. J. Prev. Vet. Med., 2024, 8(46): 791-798. (In Chinese)
26. Peng, Q.; Fu, P.; Zhou, Y.; et al. Phylogenetic Analysis of Porcine Epidemic Diarrhea Virus (PEDV) during 2020-2022 and Isolation of a Variant Recombinant PEDV Strain. Int J Mol Sci, 2024, 25(20): 10878. DOI: 10.3390/ijms252010878
27. Li, Y.; Fan, C.; Li, H.; et al. Emergence of a Highly Virulent Porcine Epidemic Diarrhea Virus (PEDV) G2c Subtype in China: Isolation, Genetic and Pathogenic Characterization, and Cross-Neutralizing Antibody Response. Transbound Emerg Dis, 2026, 2026: 3811264. DOI: 10.1155/tbed/3811264
28. Xu, H.; Wu, H.; Min, J.; et al. Effective control of the emerging PEDV G2-c variant with an inactivated autogenous vaccine. Front Vet Sci, 2025, 12: 1697499. DOI: 10.3389/fvets.2025.1697499
29. Lu, X.; Chen, C.; Wang, Z.; et al. Isolation and Characterization of Porcine Epidemic Diarrhea Virus G2c Strains Circulating in China from 2021 to 2024. Vet Sci, 2025, 12(5): 444. DOI: 10.3390/vetsci12050444
30. Zhuang, H.; Sun, L.; Wang, X.; et al. Molecular characterization and phylogenetic analysis of porcine epidemic diarrhea virus strains circulating in China from 2020 to 2021. BMC Vet Res, 2022, 18(1): 392. DOI: 10.1186/s12917-022-03481-4
31. Luo, H.; Liang, Z.; Lin, J.; et al. Research progress of porcine epidemic diarrhea virus S protein. Front Microbiol, 2024, 15: 1396894. DOI: 10.3389/fmicb.2024.1396894
32. Mannar, D.; Saville, J.W.; Sun, Z.; et al. SARS-CoV-2 variants of concern: spike protein mutational analysis and epitope for broad neutralization. Nat Commun, 2022, 13(1): 4696. DOI: 10.1038/s41467-022-32262-8
33. Liu, C.; Tang, J.; Ma, Y.; et al. Receptor usage and cell entry of porcine epidemic diarrhea coronavirus. J Virol, 2015, 89(11): 6121-6125. DOI: 10.1128/JVI.00430-15
34. Li, X.; Li, Y.; Huang, J.; et al. Isolation and oral immunogenicity assessment of porcine epidemic diarrhea virus NH-TA2020 strain: One of the predominant strains circulating in China from 2017 to 2021. Virol Sin, 2022, 37(5): 646-655. DOI: 10.1016/j.virs.2022.08.002

 doi:10.20944/preprints202605.2098.v1



35. Zhu, H.; Lou, J.; Yang, Z.; et al. STT3B promotes porcine epidemic diarrhea virus replication by regulating N-glycosylation of PEDV S protein. J Virol, 2025, 99(3): e0001825. DOI: 10.1128/jvi.00018-25
36. Wang, Z.; Yang, K.; Bi, M.; et al. Molecular characteristics and potential antigenic epitope analysis of porcine epidemic diarrhea virus in China from 2022 to 2025. Front Vet Sci, 2025, 12: 1667063. DOI: 10.3389/fvets.2025.1667063